International Journal of Minerals, Metallurgy and Materials
Volume 26, Number 10, October 2019, Page 1258
https://doi.org/10.1007/s12613-019-1867-9

One-step electrochemical reduction of stibnite concentrate in molten borax

Levent Kartal[1)], *Mehmet Barış Daryal*[2)], *Güldem Kartal Şireli*[2)], *and Servet Timur*[2)]

1) Department of Metallurgical and Materials Engineering, Hitit University, Corum 19030, Turkey

2) Department of Metallurgical and Materials Engineering, Istanbul Technical University, Istanbul 34469, Turkey

(Received: 17 April 2019; revised: 10 June 2019; accepted: 12 June 2019)

Abstract: In this study, antimony production from a stibnite concentrate (Sb_2S_3) was performed in one step using a molten salt electrolysis method and borax as an electrolyte. Electrochemical reduction of the stibnite concentrate was performed at 800°C under galvanostatic conditions and explained in detail by the reactions and intermediate compounds formed in the borax. The effects of current density (100–800 $mA \cdot cm^{-2}$) and electrolysis time (10–40 min) on cathodic current efficiency and antimony yields were systematically investigated. During the highest current efficiency, which was obtained at 600 $mA \cdot cm^{-2}$, direct metal production was possible with 62% cathodic current efficiency and approximately 6 kWh/kg energy consumption. At the end of the 40-min electrolysis duration at 600 $mA \cdot cm^{-2}$ current density, antimony reduction reached 30.7 g and 99% of the antimony fed to the cell was obtained as metal.

Keywords: molten salt electrolysis; electrochemical reduction; antimony; antimony extraction; stibnite; borax

1. Introduction

Antimony is a white frangible metal with a very weak heat and electrical conductivity that is used as a raw material in many industries as an additive for hardening and corrosion inhibition properties to alloys. In particular, antimony is used in copper, tin, and lead bearing alloys, and for increasing the strength of lead anodes [1–3].

Although, there are more than 200 kinds of antimony minerals in nature, stibnite (Sb_2S_3) is the most common and most widely used mineral in antimony production. Antimony is produced from stibnite ores as a result of a multi-stage pyrometallurgical process with high initial investment and operating costs, often involving roasting, evaporation, and carbothermic reduction steps. Firstly, a two-stage crushing process is applied to the ores for size reduction and enrichment. After crushing, the ore is prepared for flotation by being subject to ball mills and spiral classifiers. In flotation, butyl xanthate, sodium diethyldithiocarbamate and shale oil are generally used as collectors. After flotation, the sulfur of the concentrate is incinerated at around 1000°C and the antimony oxide airborne material is collected using different precipitators and filters. The reduction of the collected antimony oxide is performed at 1200°C with charcoal in reverberatory furnaces. Soda, potash and sodium sulfate are added to the charge to remove sulfur and gangue residues, and to reduce antimony volatility [4–6]. During the production of antimony using hydrometallurgical methods, antimony compounds are first leached into alkaline (Na_2S) or acidic ($FeCl_3$) solutions and then metallic antimony is produced by electro-winning. Hydrometallurgical methods are not much preferred due to reasons such as low efficiency, high operating costs, and excessive water consumption [7–8]. Metal production from sulfide compounds via electrometallurgical methods has been the focus for many years due to the low theoretical energy requirement [9–10]. The fact that metal sulfides have a very high electronic conductivity in the molten state ensures that the short circuits occurring in the electrolysis of sulfide compounds. In order to prevent the short circuits, ionic conductivity-enhancing additives are required in the electrolyte, and chlorinated and sulfide compounds are generally used [11–12].

As an alternative to conventional metal production methods, metal production from oxide/sulfide compounds using calcium chloride as an electrolyte was suggested to be possible by electrochemical reduction, without melting or

Corresponding author: Levent Kartal E-mail: leventkartal@hitit.edu.tr

dissolution, using the FFC Cambridge process, which depends on high-temperature molten salt electrolysis based on titanium production from titanium dioxide. As a result, metal production via electrometallurgy and oxide/sulfide structures gained new momentum in the late 1990s [13]. In the FFC Cambridge process, pelleted and sintered solid metal oxide/sulfide compounds are cathodically polarized and the metal solidified on the cathode. The sintering temperature, porosity, and electrolysis time have a significant effect on the conversion of the metal compounds to metal [14]. Molten salt electrolysis processes are now used in many areas such as metal [15], alloy production [16] and refining [17]. As a result of these developments, studies on electrochemical production of metal (molybdenum [9,18], titanium [19], vanadium [20], aluminum [21], tungsten [22], copper [11,23–27], and antimony [28–34]) from metal sulfides in chloride- and alkaline-based electrolytes, have been accelerated.

The antimony production from antimony sulfide via electrolysis is noteworthy in studies on antimony production using different electrolytes (Sb–Sb_2S_3 [29], NaCl–KCl–Na_2S [30], NaOH [31]). Due to the low melting point of antimony sulfide (550°C) and antimony (630°C), they are in liquid form at the reduction temperature, allowing for the fast production of metal in one step starting from sulfide compounds. Yanagase and Derge [29] studied the electrochemical reduction of antimony sulfide and obtained the highest current efficiency of 56% at 635°C in their study using the Sb–Sb_2S_3 electrolyte at different temperatures above the melting point of the antimony. Moreover, using the NaCl–KCl–Na_2S electrolyte for Sb_2S_3 reduction, Yin *et al*. [30] determined that the cathode potential shifted to more negative values and the cell voltage increased with a reduction in raw material in reduction processes at a constant current density of 500 mA·cm^{-2} at 700°C. At a current density of 500 mA·cm^{-2}, the current efficiency was 88% and the energy consumption was 1.5 kWh/kg Sb. Furthermore, Qu *et al*. [31] reduced Sb_2S_3 compounds into pellets in NaOH electrolyte at 120°C, reporting the production of powder antimony at a current efficiency of 90%.

Halide-based electrolytes used in reduction studies on oxide/sulfide compounds are operated under potentiostatic conditions considering the decomposition voltage of electrolytes. In the present study, antimony was produced from a stibnite concentrate under galvanostatic conditions in borax electrolyte, which is inexpensive and stable under electrolysis conditions. The use of an oxide-based borax electrolyte eliminates the toxic gas emission caused by halide-based electrolytes. Additionally, since a degrading compound is not used, galvanostatic conditions can be performed under experimental conditions. Another benefit of borax as an electrolyte is the low amount of impurities (FeS_2, PbS, SiO_2) within the concentrate should serve as a flux, reducing the processes required to purify the concentrate, contributing to the production of metallic antimony at technical purity. Furthermore, compared with halide-based electrolytes, such as $BaCl_2$, $CaCl_2$, and NaCl, molten borax offers a low vapor pressure, low corrosivity, and easy handling due to its stable structure at relatively high temperatures.

2. Experimental

Since the outcomes of the study were aimed at industrial application, technical quality materials were used and their properties are given in Table 1. The chemical and phase analyses of the stibnite concentrate (Sb_2S_3) obtained from Eti Bakır Halıköy İşletmeleri are also shown in Table 1.

A schematic representation of the setup and reaction cell used in the experimental studies is shown in Fig. 1. Borax was fed to the graphite crucible and heated to 800°C at a rate of approximately 10°C/min in the medium frequency induction furnace (50 kHz, 30 kW, 40 A), and was maintained at 800°C for 30 min. During the experiment, the cell was swept with 50 mL/min argon.

Table 1. Materials used in electrochemical reduction experiments

Material	Specification
Sb_2S_3 (550°C)	69wt% Sb, 1wt% Fe, 0.15wt% Pb, 0.95wt% Si, remaining wt% S
Dehydrated borax ($Na_2B_4O_7$)(743°C)	Technical grade pure
Cathode	Graphite crucible, ϕ45 mm, *h* 100 mm
Anode	Graphite rod, ϕ16 mm

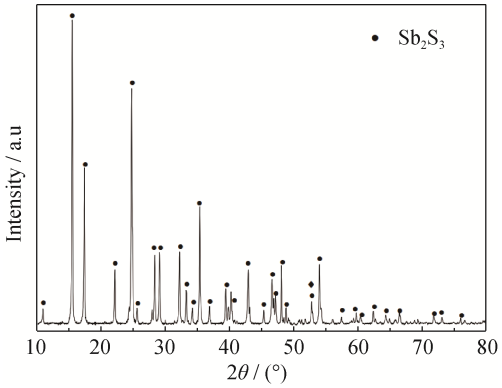

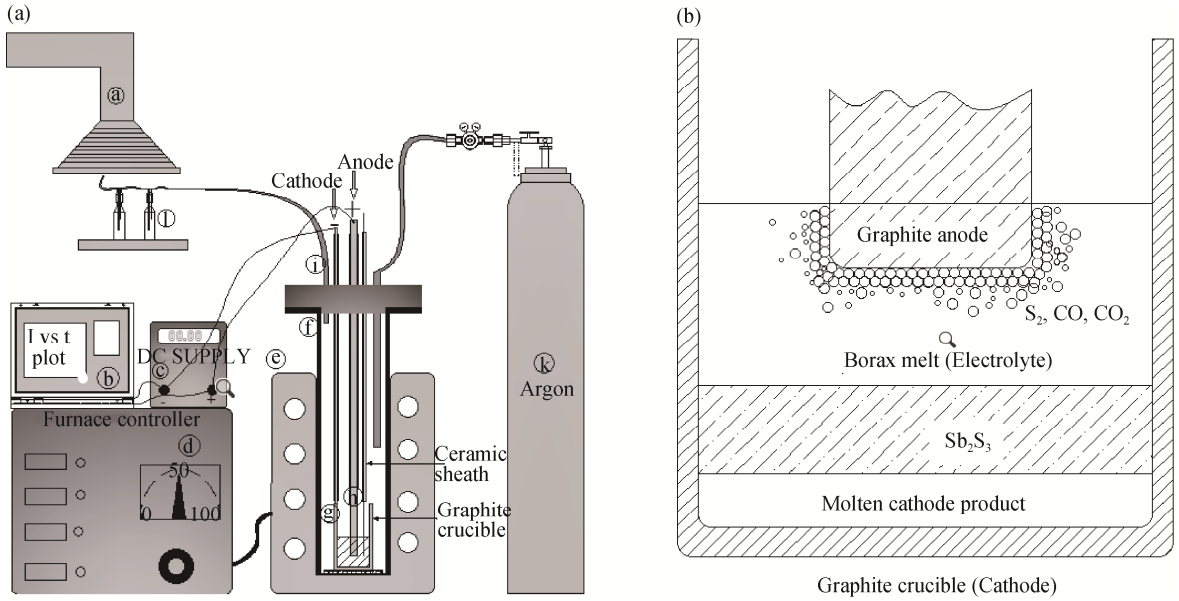

Fig. 1. Schematic illustration of the experimental setup (a) and reaction cell (b). ⓐ—Fume hood; ⓑ—Data acquisition system; ⓒ—DC supply; ⓓ—Furnace controller; ⓔ—Induction furnace; ⓕ—Alumina vessel; ⓖ—Graphite crucible cathode; ⓗ—Graphite rod anode; ⓘ—Gas outlet; ⓙ—Gas inlet; ⓚ—Argon cylinder; Ⓛ—Gas washing bottle.

The effect of time on the electrochemical reduction of stibnite concentrate in molten borax electrolyte was investigated using the same amount of homogeneous material in all experiments at a constant reaction temperature of 800°C and the most ideal current density (100−800 mA·cm^{-2}) of 600 mA·cm^{-2}. All experiments were conducted under galvanostatic conditions. The anode immersion depth was determined by considering the densities of the crucible feeds [borax electrolyte (2.4 g/cm^3)] during electrolysis, and the relative positions of the matte phase [Sb_2S_3, antimony sulfide (4.5 g/cm^3)] and antimony (6.7 g/cm^3). The anode was placed on the antimony sulfide matte in the electrolyte to prevent short circuit due to the metallic antimony.

The materials produced in the experimental studies were characterized using an X-ray diffractometer (XRD, Siemens D5000) and a scanning electron microscope with an energy-dispersive X-ray spectroscopy.

3. Results and discussion

3.1. Effects of current density on antimony yield and current efficiency

Since the amount of current is directly reduced by Faraday's Law in electrochemical reduction processes, the amount of antimony reduced at different current densities was investigated at a constant temperature of 800°C and a constant electrolysis duration of 10 min. The results are shown in Fig. 2. The antimony yield was determined by the ratio of the amount of antimony produced at the end of electrolysis to the amount of primary antimony in the antimony concentrate.

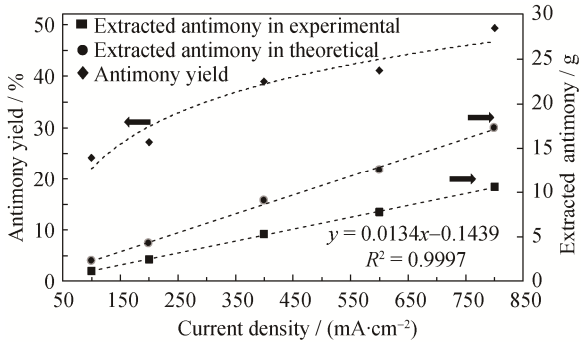

Fig. 2. Variations of antimony yield and the amounts of antimony recovery in experimental and theoretical at different current densities in molten borax at 800°C for 10 min.

Unsurprisingly, the amount of metal reduced by increasing the amount of current applied to the current density, while the current efficiency at high current densities continued to slightly increase. At low current densities, while the theoretical values remained close to each other, the difference between the theoretical and experimental values increased with an increase in current density. The empirical Eq. (1) can be generated from the amount of metal (m_{Sb}) reduced and the applied current densities (i).

$$m_{Sb} = 0.0134i - 0.1439 \quad 100 \text{ mA·cm}^{-2} \leq i \leq 800 \text{ mA·cm}^{-2}; \text{ (800°C, 10 min)} \tag{1}$$

The changes in cathodic current efficiency and energy consumption with current density are shown in Fig. 3. The

cathodic current efficiency slightly increased with increasing current density up to 600 mA·cm^{-2}; however, it did not change at 800 mA·cm^{-2} after reaching its highest value of 62% at 600 mA·cm^{-2}. In terms of possible cathodic reactions, the increasing polarization values, due to the applied current density, are more basic, but play an activating role in the reduction of sodium, which is infinite at the boundary of the electrode/electrolyte. Yanagase and Derge [29] obtained the highest current efficiency of 55% at a current density of 500 mA·cm^{-2} using an Sb−Sb_2S_3 electrolyte. In addition, in a study using a Na_2S−Sb_2S_3 electrolyte and different ratios of Na_2S, Colom and de la Cruz [32] found that the sodium ions present in the electrolyte caused a decrease in current efficiency. The literature shows that current efficiencies cannot exceed 60% with sodium ions present in the electrolyte, with the only exception to this being the work by Yin *et al*., [30], which was conducted under galvanostatic conditions and the cell voltage values were terminated by electrolysis without reaching Na_2S reduction. With respect to the relationship between current density and energy consumption in the present study (Fig. 3), these parameters continued in parallel up to 600 mA·cm^{-2}, while the current efficiency was reduced at 800 mA·cm^{-2} and the energy consumption continued to increase. Therefore, there was no need to increase the current density further, and no higher current densities were investigated.

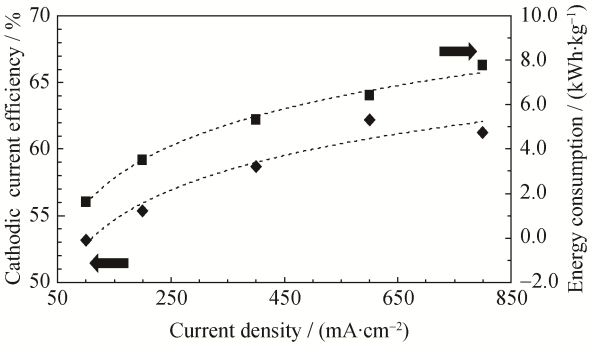

Fig. 3. Variations of cathodic current efficiency and energy consumption vs. applied current density at 800°C for 10 min.

Considering the relationship among the amount of metal reduced, cathodic current efficiency, and applied current density, the reason why the current efficiency cannot be increased further is due to the formation of Na_2S in the electrolyte together with the reduction of antimony and the resulting occurrence of Na reduction in the cathode. This situation is not specific to the borax electrolyte and also occurs with halide-based ($CaCl_2$) electrolytes of the oxide/sulfide compounds in the electrochemical reduction of intermediate compounds (solid CaV_2O_4[15], CaS [23]). Considering that a borax-based electrolyte was used and all products resulting from reduction were in the liquid form and ionic at the working temperature in accordance with the reactions (Eqs. (2)−(5)) given below, liquid Na_2S formation is possible via reaction with Na^+ at the phase boundary of the S^{2-} ions (Eq. 5) resulting from cathodic reduction. By precise XRD analysis of the antimony matte on the molten antimony, it was determined that the formed Na_2S reacted again with Sb_2S_3 in the liquid to produce $NaSbS_2$ ($Na_2S.Sb_2S_3$) (Eq. 10) in the electrolyte structure (Fig. 4). Due to cathodic reduction of the low viscosity liquid phase at the phase boundary, cathodic sodium reduction (Eq. 9) occurs, and accordingly, the effective current efficiency for antimony is not increased at the targeted rate.

Dissociation-ionization:

$$2Na_2B_4O_7 = 2Na_2B_2O_4 + 2B_2O_3 \quad (2)$$

$$Na_2B_2O_4 = 2Na^+ + B_2O_4^{2-} \quad (3)$$

$$Sb_2S_3 = 2Sb^{3+} + 3S^{2-} \quad (4)$$

$$2Na^+ + S^{2-} = Na_2S \quad (5)$$

Anode:

$$S^{2-} = 1/2S_2(g) + 2e^-, \quad \Delta G^{\ominus}_{800°C} = -474.743 \text{ kJ/mol} \quad (6)$$

$$B_2O_4^{2-} = B_2O_3 + 1/2O_2 + 2e^- \quad (7)$$

Cathode:

$$Sb^{3+} + 3e^- = Sb, \quad E^{\ominus} = -0.262 \text{ V}, \quad \Delta G^{\ominus}_{800°C} = 303.431 \text{ kJ/mol} \quad (8)$$

$$Na^+ + e^- = Na, \quad E^{\ominus} = -2.84 \text{ V}, \quad \Delta G^{\ominus}_{800°C} = 274.661 \text{ kJ/mol} \quad (9)$$

Chemical reactions:

$$Na_2S + Sb_2S_3 = Na_2S{\cdot}Sb_2S_3 \quad (10)$$

$$6Na + Sb_2S_3 = 3Na_2S + 2Sb, \quad \Delta G^{\ominus}_{800°C} = -737.005 \text{ kJ /mol} \quad (11)$$

The gas emissions that may occur in the system were examined in detail in light of thermodynamic and literature data. The ionized S^{2-} in the cathode reached the anode and was oxidized to S_2(g):

$$0.5S_2(g) + O_2(g) = SO_2(g), \quad \Delta G^{\ominus}_{800°C} = -283.576 \text{ kJ /mol} \quad (12)$$

$$2C + O_2(g) = 2CO(g), \quad \Delta G^{\ominus}_{800°C} = -413.464 \text{ kJ/mol} \quad (13)$$

$$C + O_2(g) = CO_2(g), \quad \Delta G^{\ominus}_{800°C} = -395.938 \text{ kJ/mol} \quad (14)$$

$$C + S_2(g) = CS_2(g), \quad \Delta G^{\ominus}_{800°C} = -17.814 \text{ kJ/mol} \quad (15)$$

$$2C + S_2(g) = 2CS(g), \quad \Delta G^{\ominus}_{800°C} = 235.404 \text{ kJ/mol} \quad (16)$$

In examining the possible reactions on the graphite anode surface, the formation of CS does not seem possible due to the thermodynamically positive $\Delta G^{\ominus}$ value. Although CS_2 formation seems possible due to the negative $\Delta G^{\ominus}$ value, it is unlikely to occur when CO_2 and CO are considered, which have highly negative $\Delta G^{\ominus}$ values [9]. Due to the low evaporation temperature, the easily evaporating sulfur can be discharged elementally without forming compounds at operating temperatures. The gas emission of the cell was

investigated with EDS by condensing it on the cold plate to determine the easily condensed sulfur that passed into the gas phase due to the low evaporation temperature. Since the possible carbon and sulfur oxide compounds were not able to condense on the plate, only the elemental sulfur emission was determined from the EDS results (Fig. 4(b)).

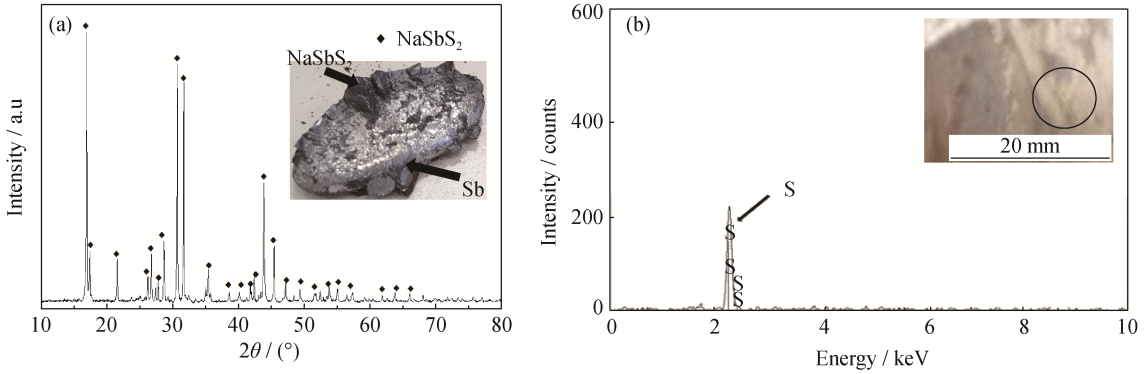

Fig. 4. XRD pattern (a) of the sodium antimony sulfide ($NaSbS_2$) and EDS analysis (b) of the condensed exhaust gases on the surface of the cold upper part of graphite crucible (current density of 600 mA·cm^{-2} at 800°C for 40 min).

In studies using halide [30] and alkaline-based [31] electrolytes for electrometallurgical antimony production, the necessity of working under the decomposition voltage of the electrolyte significantly influences the current density, and thus the production speed. Alternatively, the system developed with the use of a borax-based electrolyte has no cell potential limitations. Cell potential changes occurring with increasing current densities under galvanic conditions were recorded digitally over the course of the electrolysis period. Increasing the applied current density from 100 to 800 mA·cm^{-2} during the experiment resulted in an increase in cell voltage from 1.6 to 7.1 V, and the fluctuations (±0.3 V) became limited (Fig. 5). An unexpected voltage rise at any current density was not detected to indicate passivation.

In molten salt electrolysis processes, many factors such as the anode, cathode position, and electrode surface area can affect the cell potential. In the present study, a standard molten salt system was used, and it is possible to reduce the cell potential and unit energy consumption using a more suitable cell design [33].

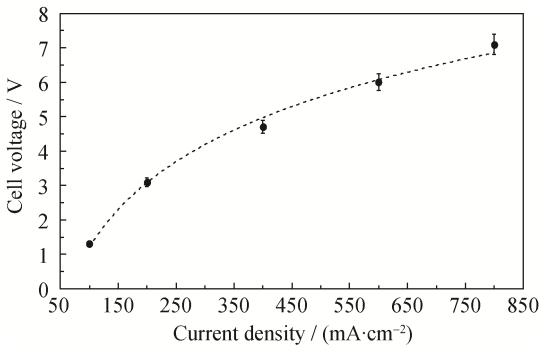

Fig. 5. Variations of cell voltage at different current densities at 800°C for 10 min.

The microstructure of the sample obtained at the highest current efficiency, at a current density of 600 mA·cm^{-2}, was examined using optical and electron microscopy, and the presence of randomly-distributed point structures in the texture was determined. Examination by EDS revealed that there were unreduced antimony sulfide structures (Table 2). The point structures contained 76% antimony and 24% sulfur, while the main matrix did not contain impurities or electrolyte contamination in the concentrate, with 100% Sb.

Table 2. EDS analysis taken from the marked points in the SEM image in Fig. 6(b) wt%

Region	Sb	S
1	76	24
2	100	0

Due to the density difference of antimony, sulfur-containing structures caused the antimony, antimony sulfide, and electrolyte to be separated by sharp boundaries; thus, the experiment was interrupted and the position of the materials in the crucible investigated. According to Fig. 7, the antimony, matte phase, and electrolyte of the material in Fig. 1(b) are in accordance with the cell design, which was formed by considering the density differences in the cell, and the density of $NaSbS_2$ (3.5 g/cm^3) caused by the chemical reaction of Sb_2S_3 with Na_2S was not a problem in the sharp separation of the phases taking place between the antimony and the borax electrolyte. Regarding the density difference from the cell cross-sectional view shown in Fig. 7, when considering the antimony, sodium antimony sulfide ($NaSbS_2$) and the electrolyte in the cell appear to be separated by sharp boundaries. The electron microscopy images

in Fig. 6 clearly show the presence of unreduced structures in the texture, which indicate that these phases entered the antimony structure by physical effects during movement inside the cell and casting to the graphite mold.

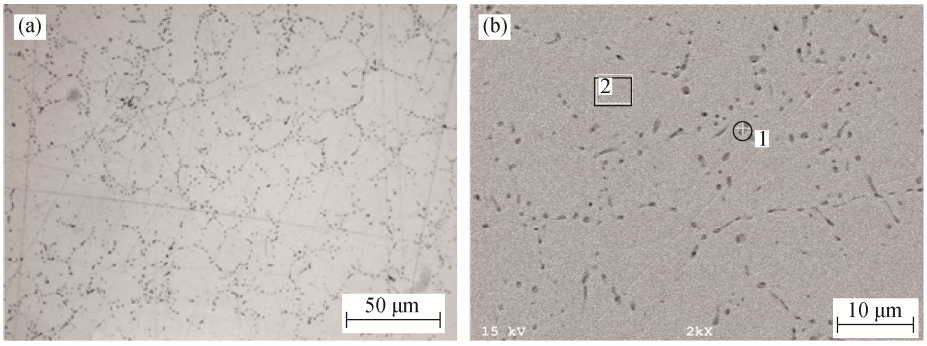

Fig. 6. Metallographic (a) and SEM (b) images of the samples synthesized at 600 mA·cm^{-2} for 10 min in molten borax at 800°C.

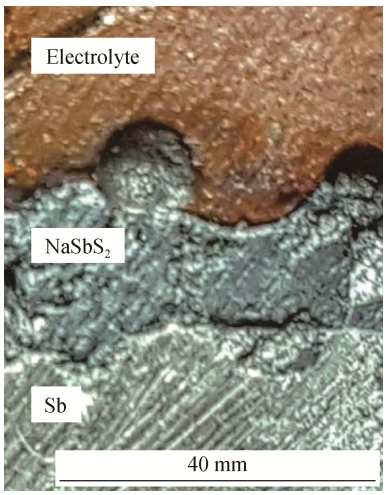

Fig. 7. Cross-sectional image of the direct electrochemical reduction cell of antimony produced from Sb_2S_3 with borax electrolyte.

3.2. Effects of electrolysis time on antimony yield

To observe the changes in anodic passivation, the current efficiency, and metal recovery efficiency that may occur over a long experimental time, the effect of electrolysis time was investigated by conducting experiments at a current density of 600 mA·cm^{-2}, corresponding to the highest current density, at 800°C for 10–40 min. During the experiments, the cell voltage was observed and no phenomena indicating anodic passivation were found. Antimony yield and the amount of metal recovered (Fig. 8) increased linearly with increasing electrolysis time, and after a 40-min electrolysis period, the antimony yield increased to 99% and the amount of antimony extraction reached 31 g.

At the end of 40 min, the structure of the cathode product obtained by reducing all if the stibnite concentrate fed to the cell was examined by electron microscopy (Fig. 9(a)) and

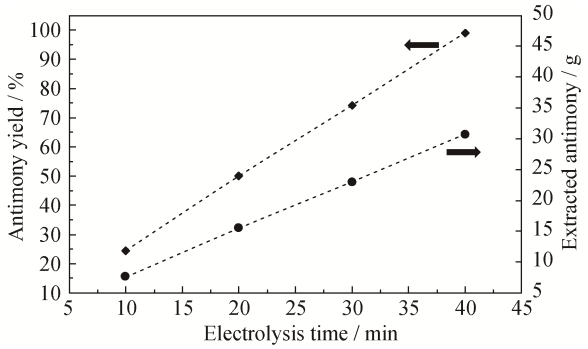

Fig. 8. Variations of antimony yield and amount of extracted antimony vs. electrolysis times at 600 mA·cm^{-2} and 800°C.

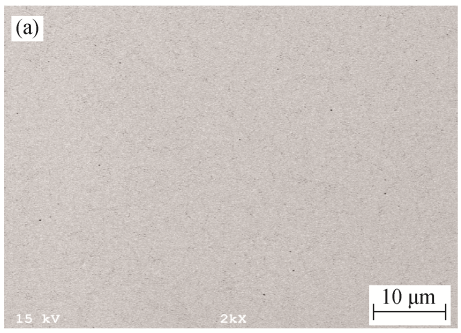

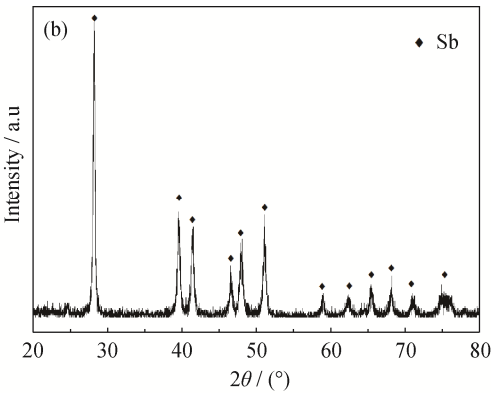

Fig. 9. SEM image (a) and XRD pattern (b) of the cathode product after 40 min of electrochemical reduction at 600 mA·cm^{-2} in molten borax at 800°C.

XRD (Fig. 9(b)). The antimony did not contain any oxidized or sulfurous impurities. As the electrolysis time was increased to 40 min, the cathode product was not contaminated by the sulfurous phases during the casting process, and the unexpected sulfurous structures that were clearly visible in Fig. 6 disappeared. This is important in terms of recognizing a sufficient time for the separation of phases in industrial production, and the fact that the molten metallic antimony is removed from the bottom of the cell and continuous metallic antimony production by the sulfurous phases is ensured.

4. Conclusions

In this study, antimony extraction from antimony sulfide using the direct electrochemical reduction method was carried out with an oxide-based borax electrolyte, which is stable under electro-reduction conditions and does not generate environmentally toxic emissions. The experimental results can be summarized as follows:

(1) During electrolysis, Na_2S formed by intermediate phase reactions, and Na_2S combined with Sb_2S_3 to form the $NaSbS_2$ melt phase and reduction was carried out through this intermediate compound.

(2) At a current density of 600 $mA \cdot cm^{-2}$, at which the highest current efficiency was obtained, antimony was produced, consuming approximately 6 kWh/kg energy with 62% cathodic current efficiency.

(3) At a current density of 600 $mA \cdot cm^{-2}$, the antimony yield reached 99% at the end of the 40-min electrolysis period, while the sulfur content of the reduced metal was zero.

(4) With borax used as an electrolyte, $NaSbS_2$ formed at the start of electrolysis, and the product was sorted by density difference. As a result, continuous production is possible without changing the electrolyte by removing antimony from the bottom.

Acknowledgements

The authors would like to thank Eti Bakır Halıköy İşletmeleri A.S for supplying stibnite concentrate.

References

[1] M. Şahin and H. Kaya, Mechanical properties of directionally solidified lead-antimony alloys, *Int. J. Miner. Metall. Mater.*, 18(2011), p. 582.

[2] Y.H. Zhao, X.B. Wang, X.H. Du, and C. Wang, Effects of Sb and heat treatment on the microstructure of Al–15.5wt%Mg_2Si alloy, *Int. J. Miner. Metall. Mater.*, 20(2013), No. 7, p. 653.

[3] J. Xie, W.T. Song, G.S. Cao, and X.B. Zhao, One-pot synthesis of Sb–Fe–carbon-fiber composites with in situ catalytic growth of carbon fibers, *Int. J. Miner. Metall. Mater.*, 19(2012), No. 6, p. 542.

[4] C.G. Anderson, The metallurgy of antimony, *Geochemistry*, 72(2012), p. 3.

[5] C. G. Anderson, *SME Mineral Processing and Extractive Metallurgy Handbook: Antimony Production and Commodites*, R. C. Dunne, S. K. Kawatra, C. A. Young, eds., Society for Mining, Metallurgy and Exploration, Englewood, 2019, p. 1557.

[6] R.S. Multani, T. Feldmann, and G.P. Demopoulos, Antimony in the metallurgical industry: A review of its chemistry and environmental stabilization options, *Hydrometallurgy*, 164(2016), p. 141.

[7] Y. Li, Y.M. Chen, H.T. Xue, C.B. Tang, S.H. Yang, and M.T. Tang, One-step extraction of antimony in low temperature from stibnite concentrate using iron oxide as sulfur-fixing agent, *Metals*, 6(2016), No. 7, p. 153.

[8] L.G. Ye, C.B. Tang, Y.M. Chen, S.H. Yang, J.G. Yang, and W.H. Zhang, One-step extraction of antimony from low-grade stibnite in sodium carbonate-sodium chloride binary molten salt, *J. Clean. Prod.*, 93(2015), p. 134.

[9] G.M. Li, D.H. Wang, X.B. Jin, and G.Z. Chen, Electrolysis of solid MoS_2 in molten $CaCl_2$ for Mo extraction without CO_2 emission, *Electrochem. Commun.*, 9(2007), No. 8, p. 1951.

[10] A. Vignes, *Extractive Metallurgy 3: Molten Salt Electrolysis Operations,* John Wiley & Sons Inc., New Jersey, 2013, p. 286.

[11] S. Sokhanvaran, S.K. Lee, G. Lambotte, and A. Allanore, Electrochemistry of molten sulfides: Copper extraction from BaS–Cu_2S, *J. Electrochem. Soc.*, 163(2016), p. 115.

[12] M.S. Tan, R. He, Y.T. Yuan, Z.Y. Wang, and X.B. Jin, Electrochemical sulfur removal from chalcopyrite in molten NaCl–KCl, *Electrochim. Acta*, 213(2016), p. 148.

[13] G.Z. Chen, D.J. Fray, and T.W. Farthing, Direct electrochemical reduction of titanium dioxide to titanium in molten calcium chloride, *Nature*, 407(2000), p. 361.

[14] Z.Q. Li, L.Y. Ru, C.G. Bai, N. Zhang, and H.H. Wang, Effect of sintering temperature on the electrolysis of TiO_2, *Int. J. Miner. Metall. Mater.*, 19(2012), No. 7, p. 636.

[15] S.L. Wang, S.C. Li, L.F. Wan, and C.H. Wang, Electro-deoxidation of V_2O_3 in molten $CaCl_2$–NaCl–CaO, *Int. J. Miner. Metall. Mater.*, 19(2012), No. 3, p. 212.

[16] P.V. Suneesh, T.G. Satheesh Babu, and T. Ramachandran, Electrodeposition of aluminium and aluminium-copper alloys from a room temperature ionic liquid electrolyte containing aluminium chloride and triethylamine hydrochloride, *Int. J. Miner. Metall. Mater.*, 20(2013), No. 9, p. 909.

[17] J.X. Song, Q.Y. Wang, G.J. Hu, X.B. Zhu, S.Q. Jiao, and H.M. Zhu, Equilibrium between titanium ions and high-purity titanium electrorefining in a NaCl–KCl melt, *Int. J. Miner. Metall. Mater.*, 21(2014), No. 7, p. 660.

[18] H.P. Gao, M.S. Tan, L.B. Rong, Z.Y. Wang, J.J. Peng, X.B.

Jin, and G.Z. Chen, Preparation of Mo nanopowders through electroreduction of solid MoS_2 in molten KCl–NaCl, *Phys. Chem. Chem. Phys.*, 16(2014), No. 36, p. 19514.

[19] N. Suzuki, M. Tanaka, H. Noguchi, S. Natsui, T. Kikuchi, and R.O. Suzuki, Reduction of TiS_2 by OS process in $CaCl_2$ melt, *ECS Trans.*, 75(2013), No. 15, p. 507.

[20] T. Matsuzaki, S. Natsui, T. Kikuchi, and R.O. Suzuki, Electrolytic reduction of V_3S_4 in molten $CaCl_2$, *Mater. Trans.*, 58(2017), No. 3, p. 371.

[21] Y. Xiao, D.W. Plas, J. Bohte, S.C. Lans, A. van Sandwijk, and M.A. Reuter, Electrowinning Al from Al_2S_3 in molten salt, *J. Electrochem. Soc.*, 154(2007), No. 6, p. 334.

[22] T. Wang, H.P. Gao, X.B. Jin, H.L. Chen, J.J. Peng, and G.Z. Chen, Electrolysis of solid metal sulfide to metal and sulfur in molten NaCl–KCl, *Electrochem. Commun.*, 13(2011), No. 12, p. 1492.

[23] X.L. Ge, X.D. Wang, and S. Seetharaman, Copper extraction from copper ore by electro-reduction in molten $CaCl_2$–NaCl, *Electrochim. Acta*, 54(2009), No. 18, p. 4397.

[24] X.L. Ge and S. Seetharaman, The salt extraction process – a novel route for metal extraction Part 2 — Cu/Fe extraction from copper oxide and sulphides, *Miner. Process. Extr. Metall.*, 119(2010), No. 2, p. 93.

[25] J.K. Qu, H.W. Xie, Q.S. Song, Z.Q. Ning, H.J. Zhao, and H.Y. Yin, Electrochemical desulfurization of solid copper sulfides in strongly alkaline solutions, *Electrochem. Commun.*, 92(2018), p. 14.

[26] H. Xie, J. Qu, Z. Ning, B. Li, Q. Song, H. Zhao, and H. Yin, Electrochemical Co-desulfurization-deoxidation of low-grade nickel-copper matte in molten salts, *J. Electrochem. Soc.*, 165(2018), No. 11, p. 578.

[27] D. Wang, C.Y. Lu, X.L. Zou, K. Zheng, Z.F. Zhou, and X.G. Lu, Electrolysis of converter matte in molten $CaCl_2$–NaCl, *J. Mater. Sci. Chem. Eng.*, 6(2018), No. 1, art. No. 82412.

[28] J.G. Yang, S.H. Yang, and C.B. Tang, The membrane electrowinning separation of antimony from a stibnite concentrate, *Metall. Mater. Trans. B*, 41(2010), No. 3, p. 527.

[29] T. Yanagase and G. Derge, Electrochemical characteristics of melts in the Sb–Sb_2S_3 system, *J. Electrochem. Soc.*, 103(1956), No. 5, p. 303.

[30] H.Y. Yin, B. Chung, and D.R. Sadoway, Electrolysis of a molten semiconductor, *Nat. Commun.*, 7(2016), art. No. 12584.

[31] J.K. Qu, X.Y. Li, H.W. Xie, Z.Q. Ning, Q.S. Song, H.J. Zhao, and H.Y. Yin, Electrochemical reduction of solid lead and antimony sulfides in strong alkaline solutions, *J. Electrochem. Soc.*, 166(2019), No. 2, p. 62.

[32] F. Colom and M. de la Cruz, Antimony electrowinning from molten sulphide, *Electrochim. Acta*, 14(1969), No. 3, p. 217.

[33] S.A. Awe and Å. Sandström, Electrowinning of antimony from model sulphide alkaline solutions, *Hydrometallurgy*, 137(2013), p. 60.

[34] Y.L. He, R.D. Xu, S.W. He, H.S. Chen, K. Li, Y. Zhu, and Q.F. Shen, Effect of $NaNO_3$ concentration on anodic electrochemical behavior on the Sb surface in NaOH solution, *Int. J. Miner. Metall. Mater.*, 25(2018), No. 3, p. 288.